Complex Formation of Amphotericin B in Sterol-Containing Membranes As Evidenced by Surface Plasmon Resonance[†]

Ryota Mouri,[‡] Keiichi Konoki, Nobuaki Matsumori, Tohru Oishi, and Michio Murata*

Department of Chemistry, Graduate School of Science, Osaka University, 1-1 Machikaneyama, Toyonaka, Osaka 560-0043, Japan

Received February 28, 2008; Revised Manuscript Received May 29, 2008

ABSTRACT: Amphotericin B (AmB) is a membrane-active antibiotic that increases the permeability of fungal membranes. Thus, the dynamic process of its interaction with membranes poses intriguing questions, which prompted us to elaborate a quick and reliable method for real-time observation of the drug's binding to phospholipid liposomes. We focused on surface plasmon resonance (SPR) and devised a new modification method of sensor chips, which led to a significant reduction in the level of nonspecific binding of the drug in a control lane. With this method in hand, we examined the affinity of AmB for various membrane preparations. As expected, AmB exhibited much higher affinity for sterol-containing palmitoyloleoylphosphatidylcholine membranes than those without sterol. The sensorgrams recorded under various conditions partly fitted theoretical curves, which were based on three interaction models. Among those, a two-state reaction model reproduced well the sensorgram of AmB binding to an ergosterol-containing membrane; in this model, two states of membrane-bound complexes, AB and AB*, are assumed, which correspond to a simple binding to the surface of the membrane (AB) and formation of another assembly in the membrane (AB*) such as an ion channel complex. Kinetic analysis demonstrated that the association constant in ergosterol-containing POPC liposomes is larger by 1 order of magnitude than that in the cholesterol-containing counterpart. These findings support the previous notion that ergosterol stabilizes the membrane-bound assembly of AmB.

Amphotericin B (AmB),[1] a polyene antibiotic produced by *Streptomyces nodosus*, is clinically used for treatment of systemic fungal infections (*1–4*). Its molecular structure (Figure 1) is characterized by a glycosylated 38-member lactone encompassing an amphiphilic polyhydroxy part, a conjugated heptaene chromophore, and an amphoteric ion pair (*5, 6*). It is generally accepted that an ion-permeable channel formed across the bilayer membrane is responsible for the biological activity of AmB (*7, 8*). In the well-known "barrel-stave" hypothesis (Figure 2), approximately eight molecules of AmB assemble to form an ion channel, where the polyhydroxy region of AmB composes the lining of a channel pore while its heptaene moiety faces the hydrophobic membrane interior (*9, 10*). The antibiotic activity of AmB is usually attributed to a higher affinity for ergosterol, a primary fungal sterol, than for cholesterol in the mammalian membranes (*11–14*). Despite extensive physicochemical investigations of this channel over many years, details of its architecture remain unelucidated except for some bimolecular interactions between AmB and AmB (*15–17*), AmB and phospholipid (*18–20*), and AmB and sterol (*21, 22*).

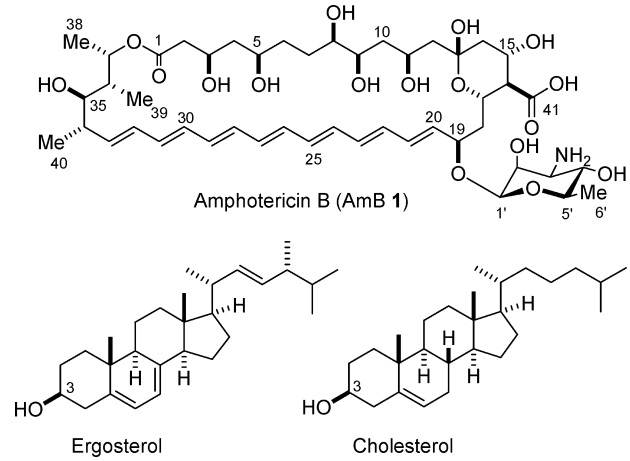

FIGURE 1: Structures of amphotericin B, cholesterol, and ergosterol.

The preference of fungus sterol over human sterol is reported to be no more than 10-fold (*13*), which is presumably responsible for the serious side effects of the drug such as nephrotoxicity or hypokalemia (*23, 24*). To develop a new drug based on the AmB skeleton with better antibiotic efficacy and fewer side effects, we must examine diverse drug candidates for membrane affinity. For this purpose, it

[†] This work was supported by Grants-in-Aid for Scientific Research (A) (15201048) and (S) (18101010), for Priority Area (A) (16073211), and for Young Scientists (A) (17681027) from MEXT, Japan. We are grateful to Japan Food Research Laboratories for generous support of R.M.

* To whom correspondence should be addressed. Telephone: +81-6-6850-5775. Fax: +81-6-6850-5785. E-mail: murata@ch.wani.osaka-u.ac.jp.

[‡] Joint Appointment with Japan Food Research Laboratories, 3-1 Toyotsu, Suita, Osaka 564-0051, Japan.

[1] Abbreviations: AmB, amphotericin B; CD, circular dichroism; DMSO, dimethyl sulfoxide; LUV, large unilamellar vesicle; MLV, multilamellar vesicle; NMR, nuclear magnetic resonance; PBS, phosphate-buffered saline; PC, phosphatidylcholine; POPC, 1-palmitoyl-2-oleoyl-*sn*-glycero-3-phosphocholine; RU, resonance unit; SPR, surface plasmon resonance.

10.1021/bi800334p CCC: $40.75
Published on Web 07/03/2008

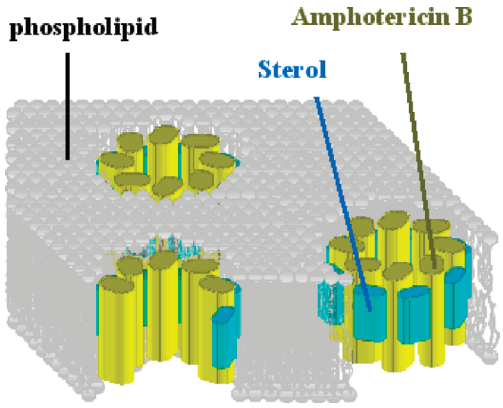

FIGURE 2: Schematic representation of the barrel-stave model for the AmB ion channel.

is particularly important to establish a simple and reliable method for quantitatively evaluating drug−membrane interaction.

Drug−membrane interaction is one of the most important subjects in pharmacokinetics (*25–31*). Nevertheless, practical methods for quantitatively evaluating the affinity of small molecules for biomembranes are rather unexploited. For drug−membrane interaction under equilibrium, calorimetric measurements (*27–29*) were successfully applied to reveal some thermodynamic properties, yet these methods are not suitable for measuring the time course of the interactions. Recently, surface plasomon resonance (SPR) has emerged as a versatile tool for assessing interactions between biomolecules (*30–34*). Membrane-bound peptides and drugs have been investigated by SPR (*32–34*), some of which produced otherwise unobtainable information about their mode of action. For cationic amphiphilic drugs such as chlorpromazine and desipramine (*32*), SPR sensor chips with a hydrophobic surface were successfully utilized to evaluate the binding affinity of these drugs for membranes. To extend this method to complex amphiphilic molecules such as amphotericin B, the level of nonspecific binding to the basis of a sensor chip, which sometimes prevents the observation of membrane interactions, has to be reduced.

In this study, we devised a new SPR method for reducing the extent of nonspecific interaction between analytes and sensor chip basis, which led to a simple, quick, and sensitive methodology for evaluating interaction between AmB and lipid bilayers. This method greatly facilitated kinetic analysis for AmB binding to sterol-containing PC membranes.

MATERIALS AND METHODS

Materials. 1-Palmitoyl-2-oleoyl-*sn*-glycero-3-phosphocholine (POPC) was purchased from NOF Corp. (Tokyo, Japan). Amphotericin B (AmB), cholesterol, chloroform, sodium chloride (NaCl), potassium chloride (KCl), disodium hydrogen phosphate, potassium dihydrogen phosphate, [3-(3-cholamidopropyl)dimethylammonio]-1-propanesulfonate (CHAPS), and cystamine dihydrochloride were purchased from Nacalai Tesque, Inc. (Kyoto, Japan). Ergosterol was purchased from WAKO Pure Chemical Industries, Ltd. (Osaka, Japan). 1-Ethyl 3-[3-(dimethylamino)propyl]carbodiimide hydrochloride (EDC), *N*-hydroxysuccinimide (NHS), 10 mM acetate buffer (pH 5.0), 1 M ethanolamine hydrochloride (pH 8.5), and 50 mM sodium hydroxide (50 mM NaOH) were purchased from BIAcore AB (Uppsala, Sweden). Dimethyl sulfoxide (DMSO) and dodecylamine were purchased from Sigma-Aldrich Co. (St. Louis, MO). All of these chemicals were of the highest grade and used without further purification. Water was purified with a Millipore Simpli Laboratory system (Millipore Inc., Bedford, MA) and used within a few hours.

Preparation of Liposomes. Large unilamellar vesicles (LUVs) were prepared according to the protocol of Herve et al. (*35*). POPC and sterol (cholesterol or ergosterol) were mixted in chloroform (1 mL) in a round-bottom flask. The mixture was evaporated and dried in vacuo for more than 2 h, and then hydrated with 10 mM phosphate buffer (pH 7.4) containing KCl (2.7 mM) and NaCl (137 mM) (PBS buffer, 1 mL). The mixture was vortexed and sonicated to prepare multilamellar vesicles (MLVs). The resultant suspension was subjected to three cycles of freezing (−80 °C), thawing (60 °C), and vortexing (5 s) to form LUVs. The LUVs were passed through double 100 nm polycarbonate filters 19 times with LiposoFast-Basic (AVESTIN Inc., Ottawa, ON) at room temperature and diluted with PBS buffer to furnish a LUV solution with a lipid concentration of 0.5 mM.

Surface Plasmon Resonance Experiments. AmB (4.62 mg, 5 μmol) was dissolved in DMSO (1 mL) and stored as a 5 mM AmB stock solution. For SPR measurements, the stock solution was first diluted with PBS buffer to 250 μM and then diluted again with PBS buffer containing 5% DMSO to give 5, 10, 20, and 50 μM AmB solutions. The experiments were performed at 25 °C using either the L1 sensor chip or the CM5 sensor chip mounted in a BIAcore X analytical system (BIAcore AB). A washing solution was comprised of 20 mM CHAPS, 40 mM cystamine, and 50 mM sodium hydroxide. After a routine pretreatment of the BIAcore instrument, the sensor chip was washed with distilled water overnight to remove trace amounts of detergent. The sensor chip surface was treated with 20 mM CHAPS (40 μL) and 40 mM cystamine (40 μL) at a flow rate of 20 μL/min. Dodecylamine was immobilized to one of the flow cell lanes in the CM5 sensor chip by an amino coupling method, while the other lane was left intact as a control lane. The immobilization reaction was performed at a flow rate of 5 μL/min; briefly, the sensor chip was activated for 7 min by injecting a solution mixture (1:1, v/v, 35 μL) of 390 mM EDC and 100 mM NHS. Dodecylamine (50 μg/mL) in 10 mM acetate buffer containing 10% DMSO (pH 5.0, 35 μL) was then injected for cross-linking. The remaining activated *N*-hydroxysuccinimide ester groups were converted to amide groups by 1 M ethanolamine hydrochloride (pH 8.5, 35 μL). The sensor chip thus obtained was washed with 10% DMSO (35 μL) to remove nonspecifically bound substances.

The running buffer was PBS buffer containing 5% DMSO (pH 7.4). Prior to being used, the buffer was passed through a 0.45 μm filter and degassed by sonication. The liposome solution (60 μL) was injected to the sensor chip at a flow rate of 2 μL/min, and then 50 mM sodium hydroxide (40 μL) was added at a flow rate of 20 μL/min. The NaOH treatment was repeated three times, resulting in a stable baseline which indicated formation of stable liposome layers on the sensor chip. AmB at various concentrations dissolved

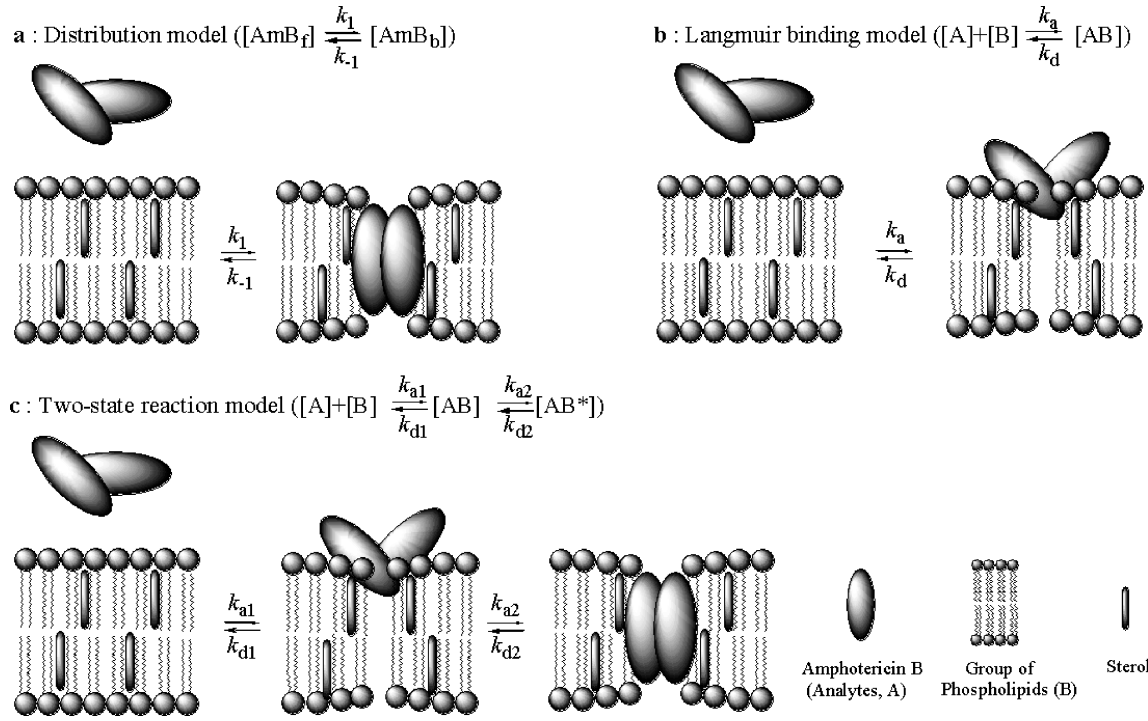

FIGURE 3: Schematic illustrations of three interaction models which may account for the binding of AmB to liposome membranes: (a) distribution model, (b) Langmuir binding model, and (c) two-state reaction model.

in the running buffer (100 μL) was introduced to the sensor chip at a flow rate of 10 μL/min, and the time course of its association and dissociation was monitored.

Data Analysis. As shown in Figure 3, we assumed three reaction models for AmB binding to liposome membranes. In the distribution model, the binding process can be expressed by two kinetic constants for phase transfer regardless of the concentration of a drug in the membrane (Figure 3a). In the Langmuir binding model, where a finite amount of receptor for drug binding is assumed, a simple model is provided by hypothesizing stoichiometric interaction between AmB (A) and a group of lipid molecules in immobilized liposomes (B) (Figure 3b). In the two-state reaction model, two steps of drug−membrane interactions are assumed. This first step where analytes (A) bind to a finite number of lipid molecules (B) is stoichiometric as is the case with the Langmuir model. The second step involves conversion from the initial complex (AB) to another complex (AB*) where interactions between the complex (AB or AB*) and uncomplexed lipids are not rate-limiting (Figure 3c) as reported for membrane-lytic peptides (*33*). Detailed descriptions of how to determine kinetic parameters on the basis of these models are given in the Supporting Information and literature (*33, 36*).

RESULTS

Newly Devised Sensor Chip for Detecting AmB−Liposome Interactions. In SPR experiments, choice of a sensor chip is particularly important. There are two types of sensor chips, L1 and HPA, which are frequently used for membrane systems; in the L1 chip, lipophilic groups are covalently attached to carboxymethylated dextran, making the surface suitable for direct attachment of liposomes, and in the HPA chip, a flat hydrophobic sensor surface consisting of long chain alkanethiol is attached directly to the gold film. The hydrophobic surface is supposed to facilitate adsorption of lipid monolayers.

The L1 sensor chips with no pretreatment were first used for interaction measurements, resulting in a large amount of nonspecific binding of AmB (Figure 4a). The CM5 chip, which consisted of carboxymethylated dextran covalently attached to a gold surface, was alkylated with dodecylamine to prepare a modified surface, which mimicked that of an L1 chip but probably possessed fewer alkyl substituents. This chip also exhibited significant nonspecific binding of AmB. On the other hand, an unmodified CM5 chip gave rise to a negligible amount of AmB bound to the chip (Figure 4b). We deduced that the hydrophobic chains of the modified CM5 (or L1) chip were responsible for the nonspecific binding of AmB. Thus, one of two flow cell lanes in the CM5 chip was modified with dodecylamine, while the other lane remained intact for the use of a control run. In the modified lane, POPC liposomes were stably captured (Figure 5). When the liposomes at a phospholipid concentration of 0.5 mM were introduced, the SPR response due to liposome association reached 15800 ± 100 RU. The sensor chip was tolerant of NaOH treatments (50 mM), and the amount of captured liposomes was essentially unchanged after repetitive use and wash. For kinetic analysis, the binding of AmB to liposome membranes was standardized as an amount of AmB in RU bound to the amount of lipids equivalent to 10000 RU.

Interaction between AmB and Liposomes on a Modified CM5 Chip. Using this newly devised sensor chip, we evaluated AmB binding to liposomes which were composed of various lipid constituents. The SPR response in the control lane was subtracted from that in the liposome-captured lane. The sensorgrams showed AmB concentration-dependent responses (Figure 6). AmB bound preferentially to sterol-containing liposomes as compared with

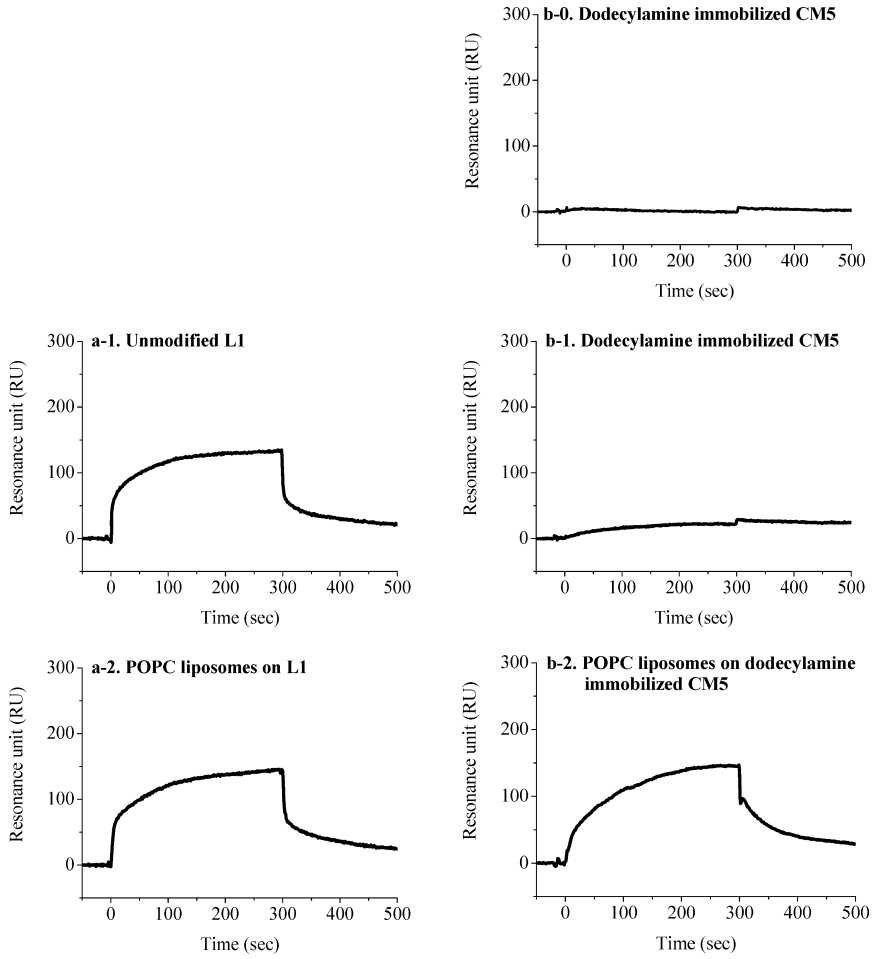

FIGURE 4: Binding of AmB (20 μM) to L1 (a-1 and a-2), unmodified CM5 (b-0), and modified CM5 (b-1 and b-2) sensor chips. Dodecylamine was immobilized on the chips of b-1 and b-2. The unmodified CM5 chip was run with the other lot of a CM5 chip; a similar sensorgram where the trace always stayed below 5 RU was obtained with the same chip that was used for for b-1 and b-2.

those of pure POPC. These marked differences unambiguously demonstrate that the drug specifically interacts with liposomes but not with the dodecylamide moiety that was introduced to capture liposomes. Thus, the RU changes upon AmB addition are largely responsible for the drug−liposome interaction. Sensorgrams for 5, 20, and 50 μM AmB solutions are shown in Figure 6a with pure POPC liposomes, Figure 6b with 20% cholesterol-containing POPC liposomes, and Figure 6c with 20% ergosterol-containing POPC liposomes. These traces clearly revealed the dose-dependent binding of AmB, where either cholesterol or ergosterol significantly increased the level of AmB binding. We next carried out kinetic analysis of the drug's binding to membrane using ORIGIN for the distribution model and BIAevaluation software for the Langumiur binding and two-state reaction models. The distribution model fits excellently the experimental sensorgram in the initial 20 s as shown in Figure 7. The plots clearly reveal that AmB binds much more efficiently to sterol-containing POPC membranes and ergosterol further enhances membrane binding as compared with cholesterol. The partition coefficients thus determined were 110 for pure POPC liposomes, 401 for 20% cholesterol-containing ones, and 1330 for 20% ergosterol-containing ones at 20 μM AmB (Supporting Information, Table S1). On the other hand, the fitting using the distribution model for a longer time period did not work well, thus suggesting that the partition coefficient depends on an amount of membrane-bound AmB (Supporting Information, Figure S1). In addition, the coefficient turned out to be influenced also by the concentration of AmB in the aqueous phase (Table S1); in particular, the association rate (k_1) markedly decreased as the concentration increased. This may be ascribed to the concentration-dependent formation of aggregates in the aqueous phase, whose size should significantly affect AmB binding to membranes. This characteristic feature of AmB prevents us from evaluating kinetic parameters in detail using the global fitting method, in which the parameters are usually determined by changing the concentration of an analyte (*36*).

Drug−Membrane Interactions As Analyzed by the Two-State Reaction Model. We then examined the other two models for their fitting to the experimental data. The Langmuir binding and two-state reaction models are based upon the stoichiometric interaction between ligands and a finite number of receptors (Figure 3). Both of the models closely mimic the experimental sensorgrams (Figure S2 of the Supporting Information). Since the two-state reaction model theoretically includes the Langmuir model (when $k_{a2} = 0$), we determine kinetic parameters of AmB binding to sterol-containing membranes on the basis of the two-state reaction model. Since the parameters appeared to depend on AmB concentration, we adopted sensorgrams at 20 μM AmB to obtain a better signal-to-

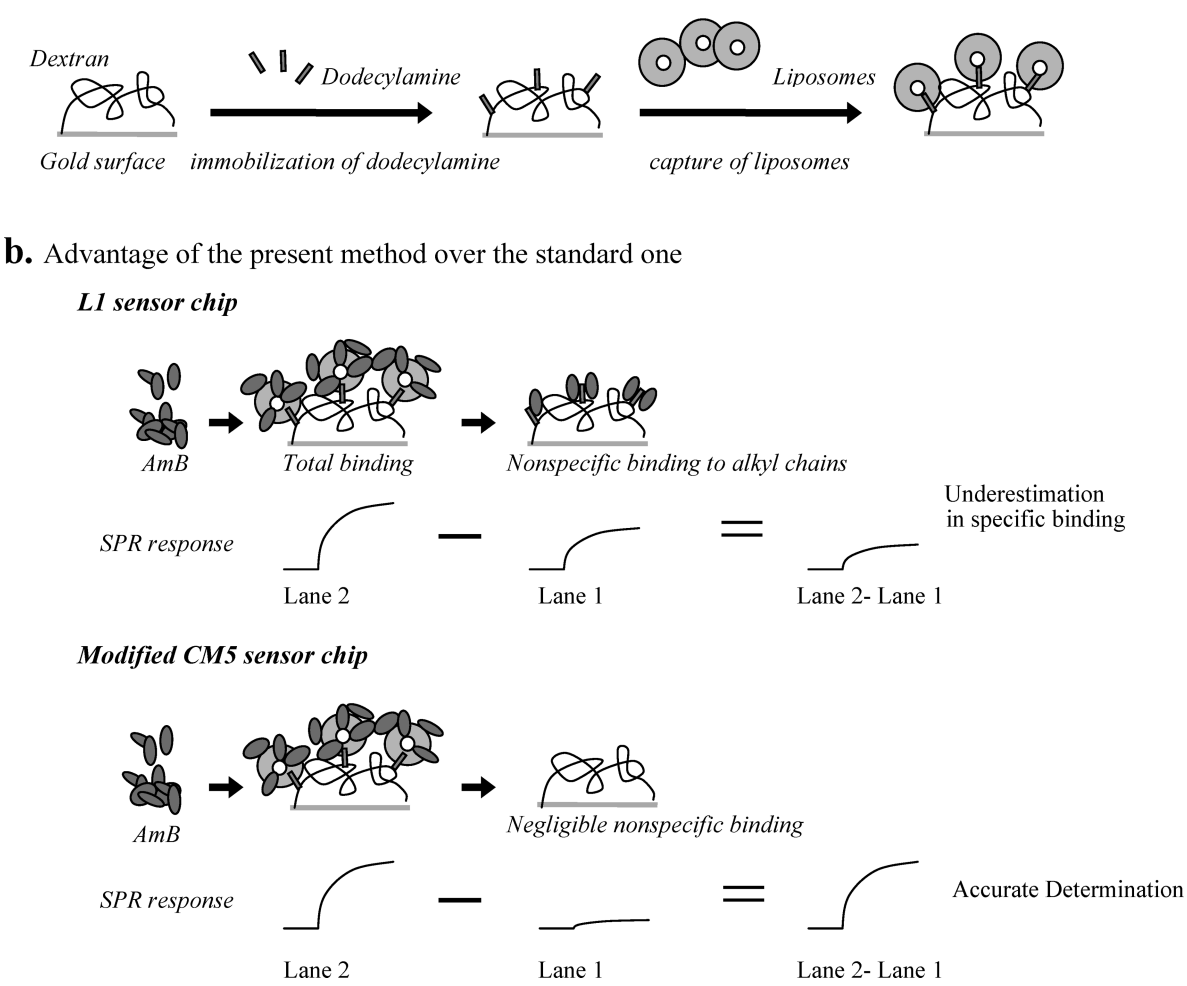

FIGURE 5: Schematic illustration of (a) modification of flow cell lane 2 in the CM5 sensor chip with dodecylamine and (b) the advantage of our method over the standard one. The alkyl chain in the L1 sensor chip showed significant nonspecific binding, yielding underestimated specific binding response (the middle scheme). There was negligible nonspecific binding in the CM5 sensor chip, yielding a more appropriate response for specific binding of AmB (the bottom scheme).

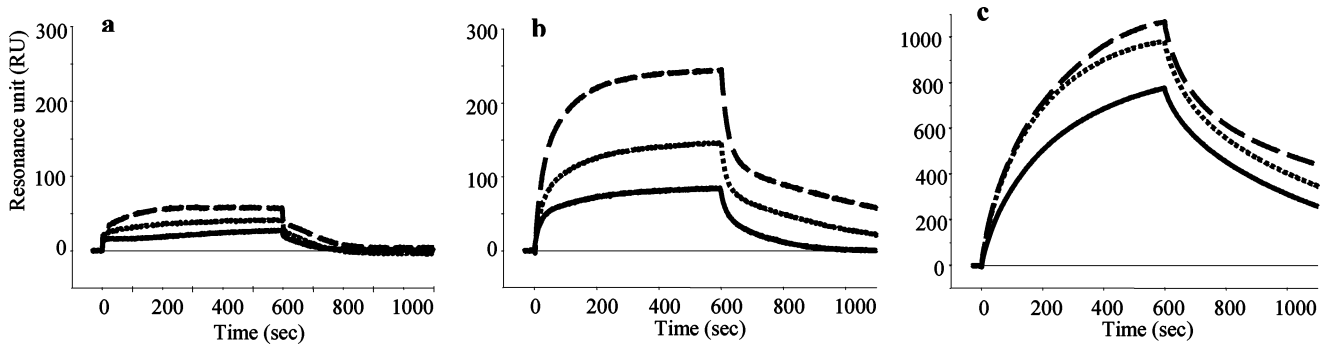

FIGURE 6: SPR sensorgrams for AmB binding to liposomes captured on the dodecylamine-modified CM5 sensor chip. (a) Pure POPC liposomes, (b) 20% cholesterol-containing POPC liposomes, and (c) 20% ergosterol-containing POPC liposomes were captured onto the dodecylamine-bound CM5 sensor chip: 5 (—), 20 (•••), and 50 μM AmB (– – –). Note the scale of the *y*-axis in panel c is different from that in panels a and b.

noise ratio and to reduce mass transport effects. In the two-state reaction model, two steps are assumed in formation of the ligand-bound complex; the first step represents the initial binding of AmB (A) to the liposome (B) by direct interaction between AmB and the head groups of POPC, and the second step corresponds to the insertion of AmB from the liposome interface into the liposome interior to form the other type of complex (AB*) that may correspond to an ion channel assembly as shown in Figure 3c. Figure 8 shows curve fitting of the SPR sensorgrams to the two-state reaction model (in the top) and three components in the two-state reaction model (in the bottom). Table 1 lists kinetic constants obtained from the analysis of AmB binding to cholesterol- or ergosterol-containing POPC liposomes as well as those for the pure POPC membrane, where k_{a2} and k_{d2} could not be accurately determined due to low binding affinity of AmB. Interestingly, the ergosterol has drastic effects on binding

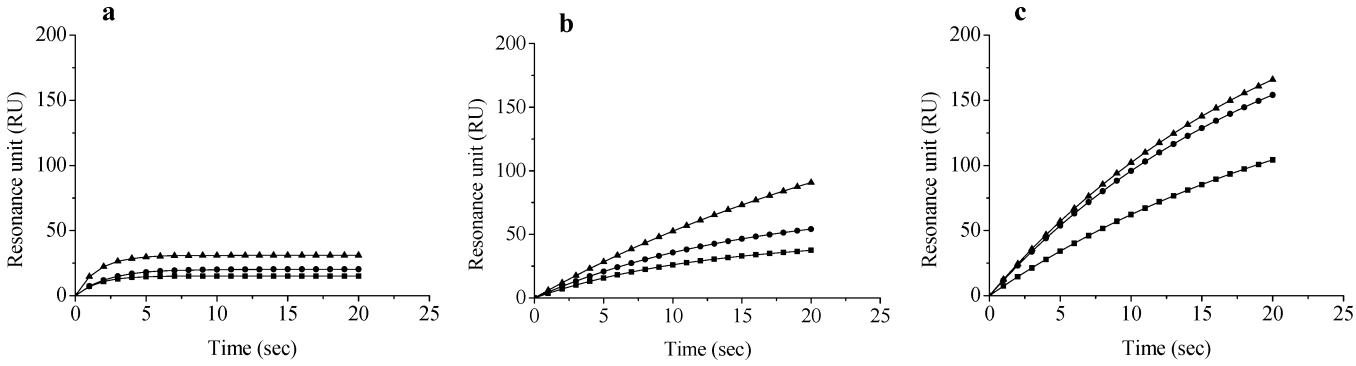

FIGURE 7: Curve fitting of the SPR sensorgrams to the distribution model: (a) pure POPC liposomes, (b) 20% cholesterol-containing POPC liposomes, and (c) 20% ergosterol-containing POPC liposomes. Experimental RU values were recorded for AmB concentrations of 5 (■), 20 (●), and 50 μM (▲) during the initial 20 s, and solid curves are theoretical ones based on the distribution model (Figure 3a).

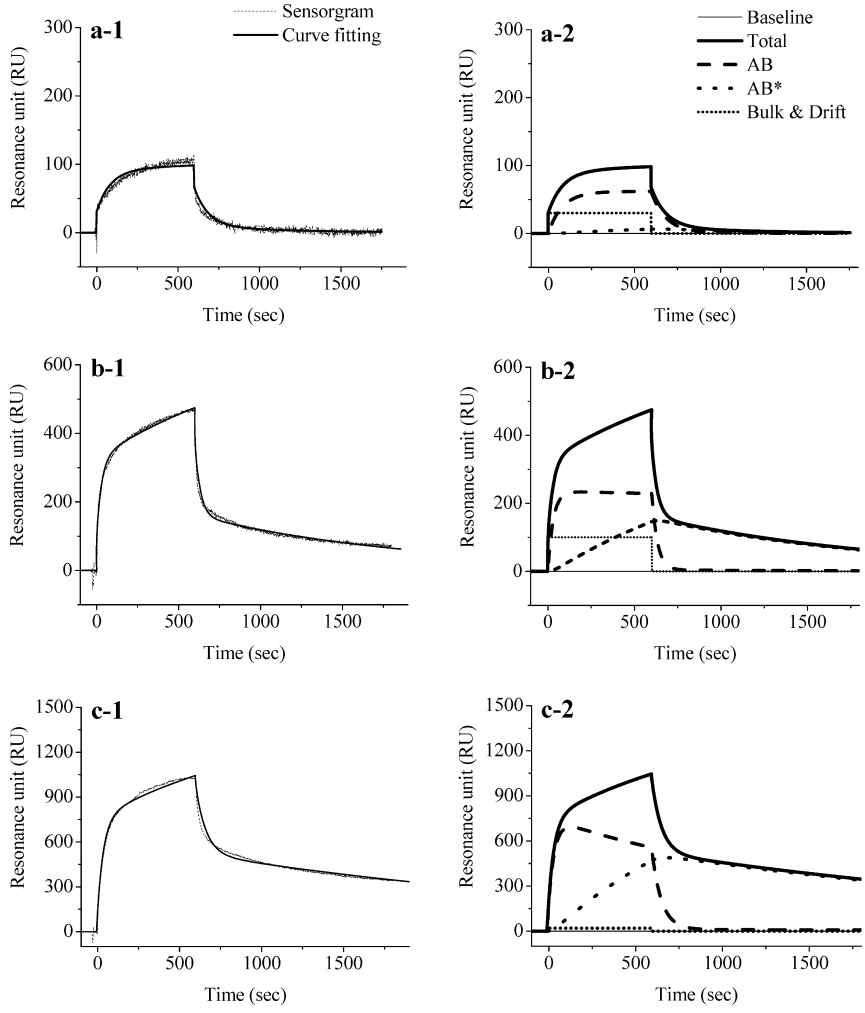

FIGURE 8: Curve fitting of the SPR sensorgrams to the two-state reaction model: (a) pure POPC liposome, (b) 20% cholesterol-containing POPC liposomes, and (c) 20% ergosterol-containing POPC liposomes. Experimental RU values were recorded for 20 μM AmB. In the top traces, a-1, b-1, and c-1, experimental sensorgrams are presented as dashed lines and theoretical curves as solid lines. In the bottom traces, a-2, b-2, and c-2, three components in the two-state reaction model are separated: (—) total, (---) AB, (•••) bulk effect of the solvent, and (— — —) AB*. Note the scales of the *y*-axis are different.

of AmB to membrane and the stability of the membrane-bound complex, AB*, as revealed by k_{a1} and k_{d2}, respectively.

DISCUSSION

In this study, we aimed to establish a simple and quick method that could be utilized in the screening of membrane-active agents. Several SPR studies have been carried out for detecting interactions of antimicrobial peptides and lipid bilayer membranes (*32-34*), most of which adopted HPA and/or L1 sensor chips. In our experiments, the strong nonspecific binding of AmB hampered the use of the L1 chip, chiefly due to the strong amphiphilicity of an AmB molecule, where hydrophobic polyene and hydrophilic polyol faces are clearly segregated. We built a novel sensor chip by modifying a CM5 sensor chip with

Table 1: Kinetic and Affinity Constants for Interaction between AmB (20 μM) and Sterol-Containing POPC Liposomes Obtained from the Two-State Reaction Model[a]

liposome/sterol	k_{a1} (M^{-1} s^{-1})	k_{d1} ($\times 10^{-2}$ s^{-1})	k_{a2} ($\times 10^{-3}$ s^{-1})	k_{d2} ($\times 10^{-5}$ s^{-1})	K_{A1} ($\times 10^{4}$ M^{-1})	K_{A2}	K_A ($\times 10^{4}$ M^{-1})
POPC	29.2	1.14	–	–	0.256	–	–
9:1 POPC/cholesterol	73.1	2.10	1.84	110	0.348	1.67	0.581
8:2 POPC/cholesterol	118	2.91	1.37	79.0	0.405	1.73	0.701
9:1 POPC/ergosterol	307	1.18	1.50	49.6	2.60	3.02	7.85
8:2 POPC/ergosterol	579	1.30	1.29	18.6	4.45	6.94	30.9

[a] The association rate constants (k_{a1} and k_{a2}), the dissociation rate constants (k_{d1} and k_{d2}), and the equilibration constants K_{A1} (k_{a1}/k_{d1}), K_{A2} (k_{a2}/k_{d2}), and K_A ($k_{a1}/k_{d1} \times k_{a2}/k_{d2}$).

dodecylamine in one of the two flow cell lanes, which markedly reduced the level of nonspecific binding of AmB. With this sensor chip in hand, we succeeded in selectively observing the interaction of AmB with sterols embedded in lipid bilayers. To the best of our knowledge, this is the first example of SPR observation of AmB−membrane interactions. We also demonstrated that AmB has higher affinity for ergosterol-containing POPC liposomes than cholesterol-containing ones (Figures 6 and 7), which is consistent with previous reports (*22, 37–39*). We performed the SPR experiments at 25 °C where POPC liposomes were in the fluid phase and sterols increased the order of POPC lipid bilayers (*40*). Thus, the enhanced affinity for sterol membranes can be ascribed to not only direct interactions as described later but also, in part, the previous observation that AmB has a higher affinity for ordered membranes than disordered ones (*37, 41*). The efficacious concentration of the drug is assumed to be at the submicromolar level, where the distribution model is potentially applicable. The markedly high affinity for ergosterol membranes, which was demonstrated in a real-time and direct manner in this study, supports the previous observations chiefly obtained from measurements of ion permeability across membranes or UV CD spectra (*22, 37–39, 42*).

We attempted to determine kinetic parameters implicated in formation of the AmB complex from the SPR experiments. We fitted sensorgrams to three different models which were usually used for membrane systems. Theoretical curves from the distribution model mimicked the experimental sensorgrams very closely during the initial 20 s (Figure 7). Fitting over a longer period with the distribution model, however, did not work well. We next compared the other two models (Figure 3b,c) which were expected to account for the drug−membrane interactions in a more realistic manner. The two-state reaction model provided significantly closer fitting, particularly for sterol-containing POPC liposomes (Figure S2). We thus hypothesized the presence of another state for AmB upon interaction with lipid bilayer membranes (Figure 9). Recently, the interaction between melittin and lipid bilayer membranes was observed by SPR experiments using HPA and L1 sensor chips and analyzed with the two-state reaction model (*34*); melittin first binds to the outer membrane surface mainly by electrostatic interactions, then penetrates into the hydrophobic interior of lipid bilayers, and eventually forms transmembrane pores by self-assembling into oligomers (*34*). AmB is also known to form an ion-permeable channel, where several molecules of the drugs assemble into an ion channel complex with ergosterol but form a different type of sterol-free channel in a cholesterol-containing membrane (*42*). We have previously disclosed that AmB elicits an all-or-none type K^+ flux in ergosterol-containing PC liposomes, implying the presence of highly conductive and stable ion channels (*43*). In either pure PC or cholesterol-containing PC liposomes, however, less conductive ion channels are dominantly formed (*43*). These previous findings agree well with our results which show that the second complex AB* assumed in the two-state reaction model is stable in the ergosterol-containing POPC liposomes; the kinetic parameters estimated in Table 1 imply that the AmB assembly in the ergosterol membrane dissociates slowly (Figure 9). It has been suggested in the previous study by Bolard et al. that the CD spectrum of membrane-bound AmB is being gradually changed over hours (*44*) and in the electrophysiological study that the mean opening time of AmB channels is markedly longer in ergosterol membranes than in cholesterol ones (*45*). These observations for ergosterol membranes support the direct involvement of ergosterol in AmB assemblies (*22, 43, 46, 47*). Moreover, the formation of complex AB*, which may be implicated in conductive ion channels, is approximately 1 or 2 orders of magnitude higher in ergosterol membranes than in cholesterol ones as depicted by the K_A values in Table 1. This difference agrees well with the different magnitudes of ion conductivity of AmB between ergosterol and cholesterol membranes (*22*). The higher affinity of AmB for ergosterol as opposed to cholesterol is caused by minute differences in their structures; one is a hydrogen bond between the 3β-OH group of sterol and the amino sugar moiety of AmB either directly or mediated by water molecules (*10, 22, 48, 49*), and the other is a van der Waals contact between AmB heptaene chromophore and hydrophobic steroid rings (*46, 48, 50*). The high affinity of AmB for ergosterol over cholesterol is explained by the presence of an additional conjugated double bond, which allows the molecular proximity necessary to maximize the van der Waals interactions with AmB (*10, 50*). The K_A value of AmB in 20% ergosterol-containing membranes exceeds that in the cholesterol counterpart by 40-fold (Table 1), which roughly corresponds to 2.3 kcal/mol. This energy stabilization may be derived from the difference in the van der Waals force between AmB and ergosterol and between AmB and cholesterol.

In conclusion, we devised a new SPR sensor chip which enabled capture of PC liposomes and facilitated kinetic analysis of interactions between AmB and phospholipid membranes. Furthermore, we were able to investigate the effects of membrane constituents on the affinity of AmB by changing the species and concentration of sterols. Our method will open the way to highly efficient screening of

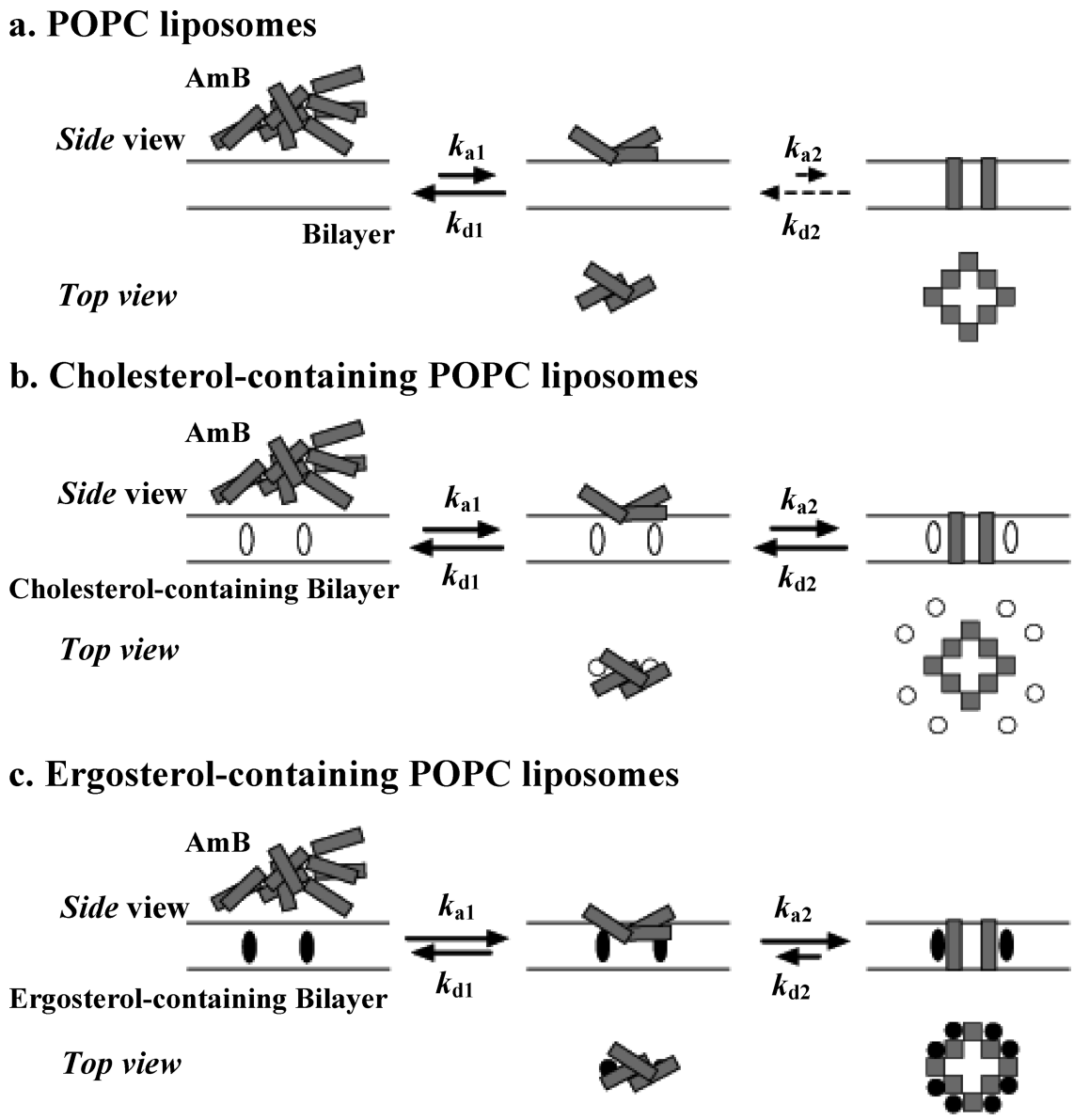

FIGURE 9: Hypothetical schemes of sterol effects as implied by the SPR results. Dynamic processes of AmB−POPC/sterol interaction can be summarized as shown in the following cases: (a) pure POPC liposomes, (b) cholesterol-containing POPC liposomes, and (c) ergosterol-containing POPC liposomes. The lengths of the arrows correspond to the magnitudes of the rate constants. The higher affinity of AmB for ergosterol-containing POPC membranes is largely ascribed to a higher association rate k_{a1} in binding to membrane and a lower dissociation rate k_{d2} in disassembling of the second complex AB*. Detailed accounts of these schemes are described in the text.

membrane-active agents and their binding affinity for biologically relevant membranes.

ACKNOWLEDGMENT

We are grateful to Toshiyuki Yamaguchi in our laboratory for discussion.

SUPPORTING INFORMATION AVAILABLE

Equations and descriptions of interaction models and additional sensorgrams used for fitting to interaction models. This material is available free of charge via the Internet at http://pubs.acs.org.

REFERENCES

1. Gallis, H. A., Drew, R. H., and Pickard, W. W. (1990) Amphotericin B: 30 years of clinical experience. *Rev. Infect. Dis. 12*, 308–329.
2. Hann, I. M., and Prentice, H. G. (2001) Lipid-based amphotericin B: A review of the last 10 years of use. *Int. J. Antimicrob. Agents 17*, 161–169.
3. Gold, W., Stout, H. A., Pagano, J. F., and Donovie, R. (1955) Amphotericins A and B, antifungal antibiotics produced by a streptomycete. I. In vitro studies. *Antibiot. Annu.,* 579–586.
4. Stemberg, T. H., Wright, E. T., and Oura, M. (1956) A new antifungal antibiotic, amphotericin B. *Antibiot. Annu.,* 566–573.
5. Mechlinski, W., Schaffner, C. P., Ganis, P., and Avitabile, G. (1970) Structure and absolute configuration of the polyene macrolide antibiotic amphotericin B. *Tetrahedron Lett. 44*, 3873–3876.
6. Ganis, P., Auitabile, G., Mechlinski, W., and Scaffer, C. P. (1971) Polyene macrolide antibiotic amphotericin B. Crystal structure of the N-iodoacetyl derivative. *J. Am. Chem. Soc. 93*, 4560–4564.
7. Bolard, J. (1986) How do the polyene macrolide antibiotics affect the cellular membrane properties? *Biochim. Biophys. Acta 864*, 257–304.
8. Hartsel, S. C., and Bolard, J. (1996) Amphotericin B: New life for an old drug. *Trends Pharmacol. Sci. 12*, 445–449.
9. De Kruijiff, B., and Demel, R. A. (1974) Polyene antibiotic-sterol interactions in membranes of *Acholeplasma laidlawii* cells and Lecithin

liposomes. III. Molecular structure of the polyene antibiotic-cholesterol complex. *Biochim. Biophys. Acta 339*, 57–70.
10. Baginski, M., Resat, H., and Borowski, E. (2002) Comparative molecular dynamics simulations of amphotericin B-cholesterol/ergosterol membrane channels. *Biochim. Biophys. Acta 1567*, 63–78.
11. Readio, J. D., and Bittman, R. (1982) Equilibrium binding of amphotericin B and its methyl ester and borate complex to sterols. *Biochim. Biophys. Acta 685*, 219–224.
12. Vertut-Croquin, A., Bolard, J., Chabbert, M., and Gary-Bobo, C. (1983) Differences in the interaction of the polyene antibiotic amphotericin B with cholesterol- or ergosterol-containing phospholipid vesicles. A circular dichroism and permeability study. *Biochemistry 22*, 2939–2944.
13. Milhaud, J., Hartmann, M., and Bolard, J. (1989) Interaction of the polyene antibiotic amphotericin B with model membranes: Differences between small and large unilamellar vesicles. *Biochimie 71*, 49–56.
14. Vertut-Croquin, A., Bolard, J., and Gary-Bobo, C. M. (1984) Enhancement of amphotericin B selectivity by antibiotic incorporation into gel state vesicles. A circular dichroism and permeability study. *Biochem. Biophys. Res. Commun. 125*, 360–366.
15. Matsumori, N., Yamaji, N., Matsuoka, S., Oishi, T., and Murata, M. (2002) Amphotericin B covalent dimers forming sterol-dependent ion-permeable membrane channels. *J. Am. Chem. Soc. 124*, 4180–4181.
16. Yamaji, N., Matsumori, N., Matsuoka, S., Oishi, T., and Murata, M. (2002) Amphotericin B dimers with bisamide linkage bearing powerful membrane-permeabilizing activity. *Org. Lett. 4*, 2087–2089.
17. Matsumori, N., Masuda, R., and Murata, M. (2004) Amphotericin B covalent dimers bearing a tertarate linkage. *Chem. Biodiversity 1*, 346–352.
18. Matsuoka, S., and Murata, M. (2003) Membrane permeabilizing activity of amphotericin B is affected by chain length of phosphatidylcholine added as minor constituent. *Biochim. Biophys. Acta 1617*, 109–115.
19. Matsuoka, S., Matsumori, N., and Murata, M. (2003) Amphotericin B-phospholipid covalent conjugates: Dependence of membrane-permeabilizing activity on acyl-chain length. *Org. Biomol. Chem. 1*, 3882–3884.
20. Matsuoka, S., Ikeuchi, H., Matsumori, N., and Murata, M. (2005) Dominant formation of a single-length channel by amphotericin B in dimyristoylphosphatidylcholine membrane evidenced by ^{13}C-^{31}P rotational echo double resonance. *Biochemistry 44*, 704–710.
21. Matsumori, N., Eiraku, N., Matsuoka, S., Oishi, T., Murata, M., Aoki, T., and Ide, T. (2004) An amphotericin B-ergosterol covalent conjugate with powerful membrane permeabilizing activity. *Chem. Biol. 11*, 673–679.
22. Matsumori, N., Sawada, Y., and Murata, M. (2005) Mycosamine orientation of amphotericin B controlling interaction with ergosterol: Sterol-dependent activity of conformation-restricted derivatives with an amino-carbonyl bridge. *J. Am. Chem. Soc. 127*, 10667–10675.
23. Cybulska, B., Gadomska, I., Mazerski, J., Grzybowska, J., Borowski, E., Cheron, M., and Bolard, J. (2000) *N*-Methyl-*N*-D-fructosyl amphotericin B methyl ester (MF-AME), a novel antifungal agent of low toxicity: Monomer/micelle control over selective toxicity. *Acta Biochim. Pol. 47*, 121–131.
24. Sedlak, M., Buchta, V., Kubicova, L., Simunek, P., Holcapek, M., and Kasparova, P. (2001) Synthesis and characterization of a new amphotericin B-methoxy polyethylene glycol conjugate. *Bioorg. Med. Lett. 11*, 2833–2835.
25. Chen, W. C., and Bittman, R. (1977) Kinetics of association of amphotericin B with vesicles. *Biochemistry 16*, 4145–4149.
26. Balon, K., Riebesehl, B. U., and Müller, B. W. (1999) Drug liposome partitioning as a tool for the prediction of human passive intestinal absorption. *Pharm. Res. 16*, 882–888.
27. Abraham, T., Lewis, R. N. A. H., Hodges, R. S., and McElhaney, R. N. (2005) Isothermal titration calorimetry studies of the binding of the antimicrobial peptide gramicidin S to phospholipid bilayer membranes. *Biochemistry 44*, 11279–11285.
28. Zhao, L., Feng, S.-S., Kocherginsky, N., and Kostetski, I. (2007) DSC and EPR investigations on effects of cholesterol component on molecular interactions between paclitaxel and phospholipid within lipid bilayer membrane. *Int. J. Pharm. 338*, 258–266.
29. Panicker, L. (2008) Interaction of propyl paraben with dipalmitoyl phosphatidylcholine bilayer: A differential scanning calorimetry and nuclear magnetic resonance study. *Colloids Surf., B 61*, 145–152.
30. Myszka, D. G., and Rich, R. L. (2000) Implementing surface plasmon resonance biosensors in drug discovery. *Pharm. Sci. Technol. Today 3*, 310–317.
31. Danelian, E., Karlén, A., Karlsson, R., Winiwarter, S., Hansson, A., Löfås, S., Lennernäs, H., and Hämäläinen, M. D. (2000) SPR biosensor studies of the direct interaction between 27 drugs and a liposome surface: Correlation with fraction absorbed in humans. *J. Med. Chem. 43*, 2083–2086.
32. Abdiche, Y. N., and Myszka, D. G. (2004) Probing the mechanism of drug/lipid membrane interactions using Biacore. *Anal. Biochem. 328*, 233–243.
33. Papo, N., and Shai, Y. (2003) Exploring peptide membrane interaction using surface plasmon resonance: Differentiation between pore formation versus membrane disruption by lytic peptides. *Biochemistry 42*, 458–466.
34. Mozsolits, H., Wirth, H.-J., Werkmeister, J., and Aguilar, M.-I. (2001) Analysis of antimicrobial peptide interactions with hybrid bilayer membrane systems using surface plasmon resonance. *Biochim. Biophys. Acta 1512*, 64–76.
35. Hervé, M., Debouzy, J. C., Borowski, E., Cybulska, B., and Gary-Bobo, C. M. (1989) The role of the carboxyl and amino groups of polyene macrolides in their interactions with sterols and their selective toxicity. A phosphorus-31 NMR study. *Biochim. Biophys. Acta 980*, 261–272.
36. Morton, T. A., Myszka, D. G., and Chaiken, I. M. (1995) Interpreting complex binding kinetics from optical biosensors: A comparison of analysis by linearization, the integrated rate equation, and numerical integration. *Anal. Biochem. 227*, 176–185.
37. Coutinho, M., and Prieto, M. (1995) Self-association of the polyene antibiotic nystatin in dipalmitoylphosphatidylcholine vesicles: A time-resolved fluorescence study. *Biophys. J. 69*, 2541–2547.
38. Castanho, M. A. R. B., Prieto, M., and Jameson, D. M. (1999) The pentaene macrolide antibiotic filipin prefers more rigid DPPC bilayers: A fluorescence pressure dependence study. *Biochim. Biophys. Acta 1419*, 1–14.
39. Bolard, J., Vertut-Croquin, A., Cybulska, B. E., and Gary-Bobo, C. M. (1981) Transfer of the polyene antibiotic amphotericin B between single-walled vesicles of dipalmitoylphosphatidylcholine and egg-yolk phosphatidylcholine. *Biochim. Biophys. Acta 647*, 241–248.
40. Hubbell, W. L., and McConnell, H. M. (1971) Molecular motion in spin-labeled phospholipids and membranes. *J. Am. Chem. Soc. 93*, 314–326.
41. Matsuoka, S., and Murata, M. (2002) Cholesterol markedly reduces ion permeability induced by membrane-bound amphotericin B. *Biochim. Biophys. Acta 1564*, 429–434.
42. Bolard, J., Legrand, P., Heitz, F., and Cybulska, B. (1991) One-sided action of amphotericin B on cholesterol-containing membranes is determined by its self-association in the medium. *Biochemistry 30*, 5707–5715.
43. Matsumori, N., Umegawa, U., Oishi, T., and Murata, M. (2005) Bioactive fluorinated derivative of amphotericin B. *Bioorg. Med. Chem. Lett. 15*, 3565–3567.
44. Bolard, J., Seigneuret, M., and Boudet, G. (1980) Interaction between phospholipid bilayer membranes and the polyene antibiotic amphotericin B. Lipid state and cholesterol content dependence. *Biochim. Biophys. Acta 599*, 280–293.
45. Brutyan, R. A., and McPhie, P. (1996) On the one-sided action of amphotericin B on lipid bilayer membranes. *J. Gen. Physiol. 107*, 69–78.
46. Kasai, Y., Matsumori, N., Umegawa, Y., Matsuoka, S., Ueno, H., Ikeuchi, H., Oishi, T., and Murata, M. (2008) Self-assembled amphotericin B is probably surrounded by ergosterol: Biomolecular interactions as evidenced by solid-state NMR and CD spectra. *Chem.—Eur. J. 14*, 1178–1185.
47. Fournier, I., Barwicz, J., and Tancrede, P. (1998) The structuring effects of amphotericin B on pure and ergosterol- or cholesterol-containing dipalmitoylphosphatidylcholine bilayers: A differential scanning calorimetry study. *Biochim. Biophys. Acta 1373*, 76–86.
48. Baran, M., and Mazerski, J. (2002) Molecular modeling of amphotericin B-ergosterol primary complex in water. *Biophys. Chem. 95*, 125–133.
49. Langlet, J., Berges, J., Caillet, J., and Demarret, J.-P. (1994) Theoretical study of the complexation of amphotericin B with sterols. *Biochim. Biophys. Acta 1191*, 79–93.
50. Baginski, M., and Borowski, E. (1997) Distribution of electrostatic potential around amphotericin B and its membrane targets. *THEOCHEM 389*, 139–146.

BI800334P